World Academy of Science, Engineering and Technology
International Journal of Mechanical and Mechatronics Engineering
Vol:7, No:4, 2013

Modeling and Simulation of Delaminations in FML Using Step Pulsed Active Thermography

S. Sundaravalli, M. C. Majumder, G. K. Vijayaraghavan

Abstract**—**The study focuses to investigate the thermal response of delaminations and develop mathematical models using numerical results to obtain the optimum heat requirement and time to identify delaminations in GLARE type of Fibre Metal Laminates (FML) in both reflection mode and through-transmission (TT) mode of step pulsed active thermography (SPAT) method in the type of nondestructive testing and evaluation (NDTE) technique. The influence of applied heat flux and time on various sizes and depth of delaminations in FML is analyzed to investigate the thermal response through numerical simulations. A finite element method (FEM) is applied to simulate SPAT through ANSYS software based on 3D transient heat transfer principle with the assumption of reflection mode and TT mode of observation individually.

The results conclude that the numerical approach based on SPAT in reflection mode is more suitable for analysing smaller size of near-surface delaminations located at the thermal stimulator side and TT mode is more suitable for analysing smaller size of deeper delaminations located far from thermal stimulator side or near thermal detector/Infrared camera side. The mathematical models provide the optimum q and T at the required MRTD to identify unidentified delamination 7 with 25015.0022W/m^2 at 2.531sec and delamination 8 with 16663.3356 W/m^2 at 1.37857sec in reflection mode. In TT mode, the delamination 1 with 34954W/m^2 at 13.0399sec, delamination 2 with 20002.67W/m^2 at 1.998sec and delamination 7 with 20010.87 W/m^2 at 0.6171sec could be identified.

Keywords**—**Step pulsed active thermography (SPAT), NDTE, FML, Delaminations, Finite element method.

I. Introduction

OLDEN days, aircraft panels were made of metallic materials, such as aluminum, titanium, beryllium etc. They led to increase fuel consumption due to increased weight. Then, the concept of effective and efficient usage of materials in manufacturing of aircraft panels was slowly emerged by using alloys of aluminum, titanium and beryllium with reduced weight and cost. Inherent complexity in manufacturing such alloys led researchers to move from metallic materials to composite materials. The composite materials play an important role in heavy duty applications because of reduced weight and cost-effective. The use of composite materials in manufacturing of aircraft panels was alike alloys of metallic materials.

S.Sundaravalli is with the Department of Mechanical Engineering, M.A.M. College of Engineering, Trichy, India (Phone: +91 - 9655591999; e-mail: ss04valli@yahoo.co.in).

M. C. Majumder is with the Department of Mechanical Engineering, National Institute of Technology, Durgapur, India (e-mail: manik_rec@yahoo.com).

G. K. Vijayaraghavan is with the Department of Mechanical Engineering, Cauvery College of Engineering and Technology, Trichy, India (e-mail: haigkv@yahoo.com).

First time, in 1980s, the Delft University of Technology developed a new type of composite called Fibre Metal Laminates (FML) for making aircraft panels [1].

Defects may be produced either during manufacturing of FML or bonding composite layers with aluminum sheets, handling, or under service conditions [28]. Defects include air gap (disbonds) and foreign particles inclusions (intrusion), fibre misalignment, fibre failure, thickness variations, delaminations etc. [23]. Disbonds and delaminations between composite layers are common defects in many of aircraft panels manufacturing industries. A good assessment of such defects is essential as they may have adverse effects on the performance and safe operation of aircrafts. Usually, these anomalies are identified and characterized by various non-destructive testing and evaluation (NDTE) techniques. Infrared thermography (IRT) is one of several NDTE techniques and it essentially uses the abnormal temperature distribution on the surface of the specimen to detect and characterize defects present in composite structures [16].

Thermography is a non-destructive, non-contact and non-intrusive inspection technique that involves mapping of surface temperatures distribution of the structure to assess the subsurface features of the structure or behavior of the system. Thermography has been successfully applied over the decades to evaluate the integrity of materials, joints, electrical connections in a wide range of industrial as well as in detection of delaminations in layered structures, hidden corrosion in metallic components, cracks in ceramics and metals, voids, impact damage and inclusions in composite materials [12], [18], [7], [11], [27].

II. Literature Review

Fibre metal laminates are a new family of hybrid materials consisting of thin metal layers bonded together by fibres embedded in an adhesive [6]. As a result of this build-up, FML possess a mixture of the characteristics of both metals and FRP materials. A GLARE is a GLAss-REinforced composite in the type of FML which was mainly used in Airbus A380 super jumbo in 2001. The internal flaws called defects are invisible on the surface of the structure which may be produced during manufacturing, handling and under service conditions which may lead to unavoidable accidents. Therefore, a proper assessment of defects is required to make them use safely. Under many literature reviews, some of thermographic investigations were carried on FMLs, such as nondestructive evaluation of damage assessment in FMLs using ultrasonic and eddy current inspection [4], the influence of cooling rate on the fracture properties of a thermoplastic-

based FMLs [5], applications of an aluminium–beryllium composite for structural aerospace components [22], modelling of FML for simulation of the inter rivet buckling behaviour in a stiffened fuselage shell [19]. The numerical results were compared to the experimental data both qualitatively and quantitatively, non-destructive evaluation of aerospace materials with lock-in thermography [13], numerical modelling for thermographic inspection of FMLs by both flash pulsed and lock-in thermography [11] and the influence of disbond damage on Lamb wave propagation in GLARE composites [20].

A two dimensional (2D) finite element modeling (FEM) was used for analysing the delamination parameter effects in a composite flat plate setup in which the delaminations were produced using Teflon and other artificial inserts [9]. The possibility of identifying the defect type was demonstrated in complex structure CFRP samples inspected by thermography using experimental and FEM results [14]. The author applied both pulsed and lock-in thermography for the detection of delaminations in FML made by E-glass fibre and Aluminium metal laminates using combined experimental and FEM approach [11]. The researcher conducted experiments on GRP pipes for analysing delaminations using step pulsed active thermography (SPAT) [27]. The active thermography approaches, such as pulsed thermography and vibrothermography were employed in order to detect simulated delamination (inserts), as well as impact damage on GLARE composite panels [8]. The investigations arrived from above mentioned literatures concluded that the thermography could be used in the rapid investigation of GLARE composites, producing interpretable results.

Few works, such as [15] and [27] were only reported on SPAT method under reflection mode for analysing GRP pipes. The above-mentioned literatures show that SPAT of IRT is an effective tool for detecting delaminations in GRP pipes. The researcher [25] presented results from a study aimed at developing a novel thermochromic liquid crystal (TLC) temperature measurement system that uses light transmission instead of light reflection to measure surface temperature fields. The author [18] aimed to develop a non-destructive tool for the evaluation of bonded plastic joints. In addition, the literature [29] was only focused to analyze defects such as delaminations and disbonds in through-transmission mode of active IRT. The paper examined IRT of both transmission and reflection modes imaging and validated the feasibility of the thermal NDT approach for this application. The results of transmission mode were shown to provide greater accuracy over the reflection mode in defect depth estimation. The research [26] was presented a novel way to inspect local wall thinning in metal tubes with IRT both numerically and experimentally. The numerical analyses were carried out in both transmission and reflection modes using simulations. The concepts of reflection mode and TT mode of SPAT led the author to apply in FML for investigating delaminations. In addition, it was found that no indicative work was carried out on FML aircraft structures in both modes of observation of SPAT using a FEM for analyzing delaminations. Hence, the current study focuses to analyse the effect of size(s) and depth of delaminations on applied heat flux by time using SPAT method and develop mathematical models from numerical results to obtain the optimum heat requirement (q) and time to identify delaminations (T).

In SPAT method**,** the heat pulse is applied on the surface of the specimen for longer time duration, normally a few seconds [12] for the effective investigation of delaminations. The thermal contrast (ΔT) at specific time during heating was numerically obtained for analysing the thermal response of delaminations. ΔT is the temperature difference between defective region over non-defective region defective region in reflection mode and it is reversed in TT mode. The maximum resolvable temperature difference (MRTD) for the most of the available thermal imager (IR camera) is around $0.1^{o}C$ [3] which is chosen as a threshold value for this analysis to investigate/identify the delaminations in FML structures. Therefore, MRTD value of $0.1^{o}C$ is set as the required ΔT as the justification factor for investigating delaminations.

III. Methods of IRT

IRT techniques are classified into two types based on the temperature difference produced to obtain thermal image: passive thermography and active thermography. In a passive thermography, no external heat stimulant is used to produce sufficient surface temperature difference for analysing the abnormality present in FML aircraft structure. The temperature difference naturally exist in the structure is used to analyse delaminations. In active thermography, an external energy is applied to generate meaningful ΔT that will yield to identify subsurface delaminations [4]. This energy can be either thermal or mechanical and can be deployed using different ways, such as flash heating, step heating, lock-in thermography (LT) and vibrothermography (VT). SPAT is a kind of active thermography using step heating which was pioneered by Milne and Reynolds in the early 1980s, developing earlier work that has established the value of infrared techniques for delaminations analysis [21]. In this technique, a continuous heat flux is applied on a specimen by a powerful lamp and the observation of thermal wave heat intensity reflecting from delaminations in reflection mode and heat intensity reaching the rear surface of the specimen in TT mode. The surface temperature of defective and non-defective regions is recorded by an infrared thermal imager/infrared camera to obtain ΔT for the result analyses.

There are two common modes of SPAT: reflection and through-transmission. In the former mode, the heat source and IR camera are situated at the same side and the reflected thermal wave effect on the surface temperature is continuously monitored. The latter mode needs to access the rear surface of the sample. In the reflection mode, both the camera and heating sources are located on the front side [10]. Figs. 1 (a) and (b) depict the basic principle of through-transmission and reflection methods of observations [24]. In this study, delaminations in FML aircraft structure are analyzed by SPAT approach in both reflection and TT modes.

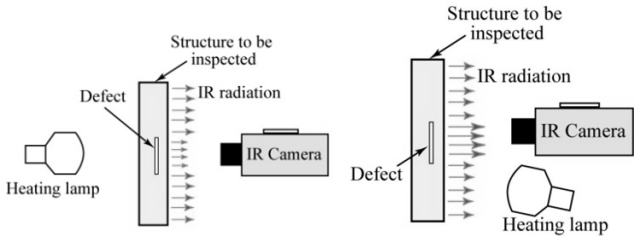

(a) Transmission method (b) Reflection method

Fig. 1 Methods of IRT [29]

IV. Numerical Modelling

FEM is mostly used to simulate thermal behaviour of materials containing delaminations. FEM is a powerful numerical tool that enables the solution of complex nonlinear, non-symmetrical mathematical problems governed by partial differential equations, such as one of heat transfer by conduction, convection and radiation with temperature dependent thermal properties of material involved [28].

For this study, the transient heating of FML structure with delaminations of varying size(s) at various depths was numerically simulated using FEM to observe the thermal response. FEM simulations were carried out using the ANSYS package.

A. Model of FML Structure and Material Properties

TABLE I
Dimensions of Delaminations [29]

Delamination No.	Size(s), mm	Depth, mm (from base)
1	2.5×2.5	0.45
2	5×5	0.45
3	7.5×7.5	0.45
4	10×10	0.45
5	12.5×12.5	0.45
6	15×15	0.45
7	2.5×2.5	0.6
8	5×5	0.6
9	7.5×7.5	0.6
10	10×10	0.6
11	12.5×12.5	0.6
12	15×15	0.6

For this study, a FML was modelled with three glass-fibre reinforced epoxy (GRE) laminates of 200×115×0.15mm placed one over the other bonded between aluminum laminates of 200×115×0.3mm of one at the top and the other one at the bottom. A model was considered for modeling delaminations in FML with the assumption of artificially induced Teflon film delaminations of 0.045 mm thick. They are numbered from 1 to 6 locating at 0.45mm depth in the thermal stimulator side and delaminations from 7 to 12 are numbered for the location at 0.6mm depth, as shown in Fig. 2.

Table II shows the thermal properties of Al 2024-T3, GRE, and Teflon taken from the literatures [11], [6], [24]. The properties of GRE are taken for the fibre volume fraction of 60% which is most commonly used for GRE composite materials.

TABLE II
Thermal Properties of Al 2024-T3, GRE and Teflon [29]

Properties	Thermal Conductivity (W/m°C)	Specific Heat (J/kg°C)	Density (kg/m^3)
Al 2024-T3	121	875	2780
Glass-fibre at 0°	0.845	840	1960
Glass-fibre at 90°	0.48	840	1960
Teflon	0.252	1043	2150

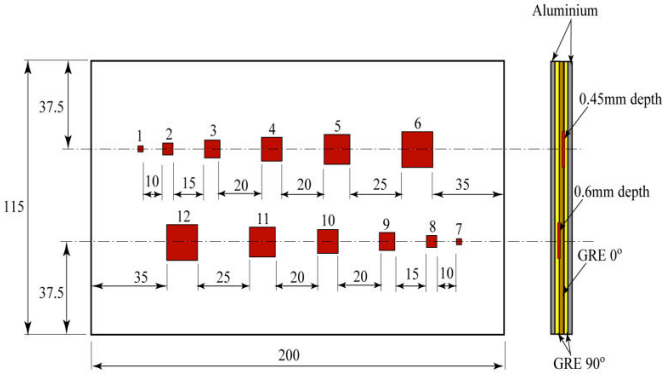

Fig. 2 A model of FML with delaminations [29]

B. Element Description

The model was meshed using 3D thermal solid elements. 8-node quadrilateral elements were used. In particular, SOLID70 elements were selected from ANSYS library. The reason of selecting SOLID70 is that 8-node elements have compatible temperature shapes. 8-node thermal element is applicable to 3D, transient thermal analysis [2], [27]. In order to obtain a good description of the heat transfer process around delaminations, mapped meshing was used instead of automatic meshing to create a fine mesh at defective regions.

C. Loading and Boundary Conditions

In reflection mode, the top surface of FML was subjected to a uniform q ranging from 1500 W/m^2 to 12000 W/m^2. The side surfaces and rear surface of the models were considered to be adiabatic in reflection mode of observation [3], [28]. In TT mode, the front surface of FML was subjected to a uniform q ranging from 10000 W/m^2 to 20000W/m^2. The reason of choosing more q is due to more distance travelled by thermal waves after crossing delaminations in such way to produce sufficient ΔT for the effective identification of delaminations. The rear surface of the model was retained to convection boundary with a convection heat transfer coefficient of h = 10W/m^{2}K [17]. Only, the side surfaces of the model were considered to be adiabatic [23]. The ambient temperature was set at 28°C in both modes. The differences resulting from applying the radiation conditions was so small as to not affect the surface in any quantifiable manner. Therefore, the effects of radiation and convection can be ignored [9], [28] in these cases. Fig. 3 shows the image taken from Ansys simulation in reflection mode. It does clearly indicate the delaminated region and non-delaminated region.

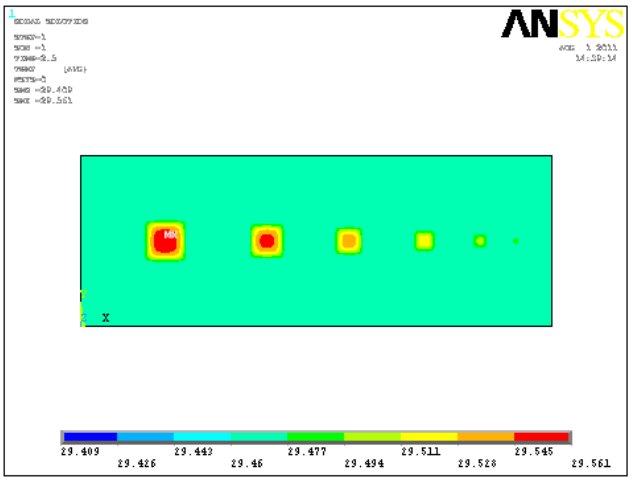

Fig. 3 Simulated Ansys image

V. Results and Discussions

In reflection mode, the temperature of the delaminations at the thermal stimulator side was measured at its centre but it was measured at the rear side of model in TT mode. In both modes, the vicinity of the delaminations was measured for non-delaminated regions. ΔT curves were drawn for the analysis during step heating in both modes obtained from simulations. The investigations were based on the thermal response, such as thermal contrast (ΔT) to attain the required MRTD with applied (q).

A. Effect of Delamination Sizes on Applied Heat Flux

In reflection mode, the results shown in Fig. 4 illustrate that ΔT of delaminations from 1 to 6 varies with time for various sizes. During the initial period, ΔT increases nonlinearly with time and it remains almost constant thereafter. ΔT curves are similar and shifted one above the other for delaminations from 1 to 6 but mainly the initial shift is more than the shift between the last three delaminations 4, 5 and 6. The reason is that the larger delaminations will provide more thermal barrier due to wide area of delaminations. Due to this, the surface above delaminations is more warmed up by resulting in the increase in surface temperature. It indicates that larger delaminations need less q to attain the required MRTD.

Similar analysis was carried in TT mode. In this case also, ΔT of delaminations from 1 to 6 varies with time for various sizes when q of 12000W/m^2 is applied, as shown in Fig. 5. The similar behavior of reflection mode was observed in TT mode. It is inferred that delamination 1 and delamination 2 produce the maximum ΔT of 0.0385^{o}C and 0.0783^{o}C respectively which are insufficient to identify them.

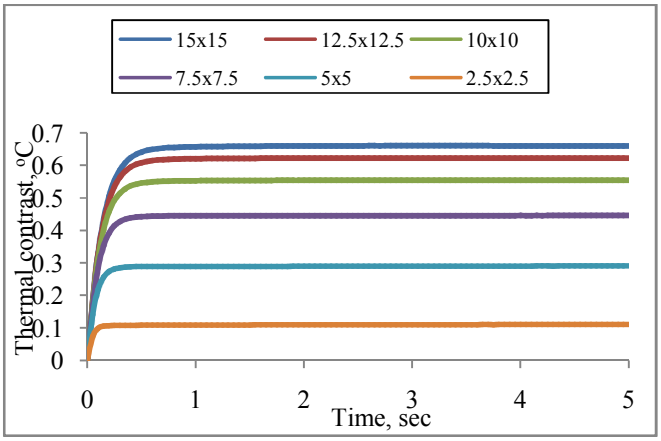

Fig. 4 Thermal contrast curves for delaminations 1 to 6 with time for 12000W/m^2 in reflection mode

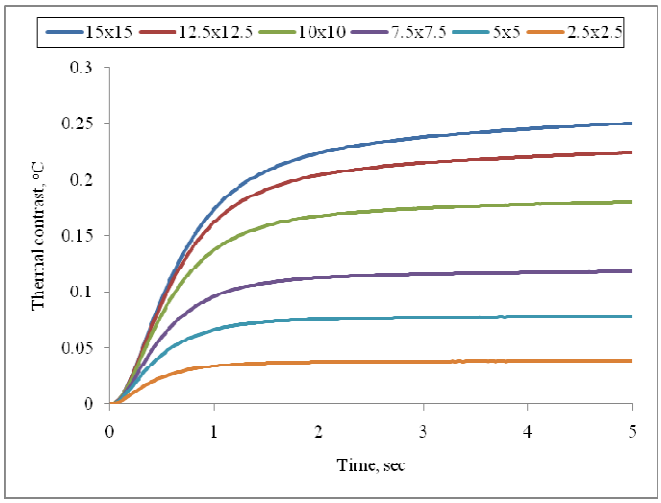

Fig. 5 Thermal contrast curves for delaminations 1 to 6 with time for 12000W/m^2 in TT mode

Fig. 6 indicates that ΔT increases nonlinearly with time for the first 2sec and it remains almost constant with slight instability thereafter for delaminations from 7 to 12 in reflection mode. Here also, ΔT curves are placed one above the other similar to delaminations from 1 to 6 but the pattern of ΔT curves do not follow the same pattern of delaminations 1 to 6, as shown in Fig. 4. It is due to the change in thermal conductivity of GRE at 0^o fibre orientation because the delaminations 1 to 6 are located at GRE 90^o fibre orientation, as shown in Fig. 2. The value of ΔT for delaminations 7 to 12 is less when compared to delaminations 1 to 6. The reason for low ΔT is that the distance covered by thermal waves to reach the delaminations is more than delaminations 1 to 6. Therefore, the reflected thermal waves from delaminations reaching the thermal imager get delayed thereby leading to reduce its surface temperature. From the analysis, it is understood that delamination 7 and delamination 8 do produce 0.0809^{o}C and 0.0544^{o}C which are not sufficient to identify them.

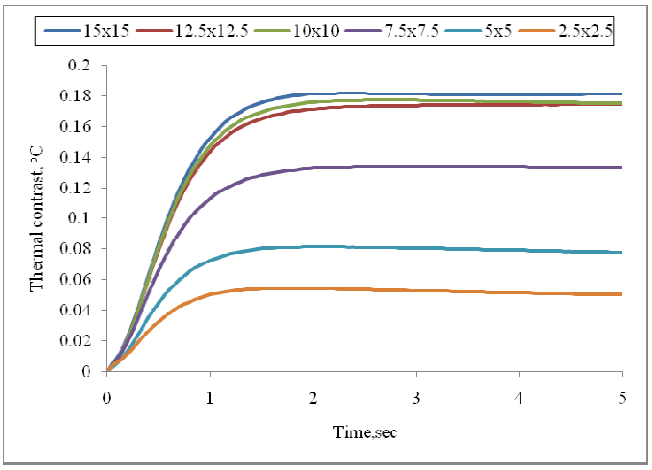

Fig. 6 Thermal contrast curves for delaminations 7 to 12 with time for 12000W/m^2 in reflection mode

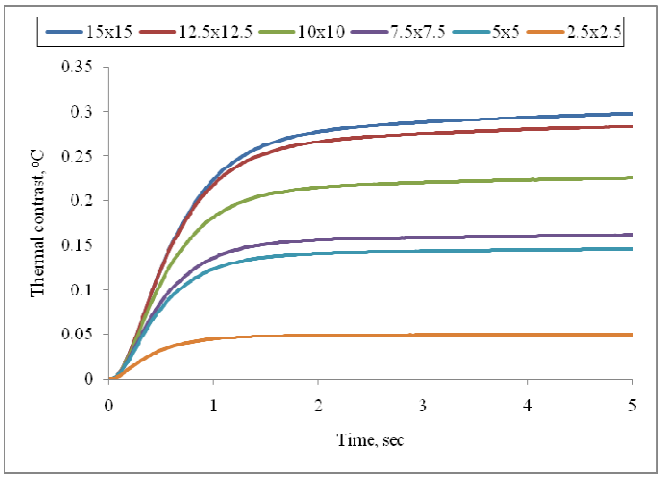

Fig. 7 Thermal contrast curves for delaminations 7 to 12 with time for 12000W/m^2 in TT mode

Similar behavior was observed in TT mode with the same reason mentioned for the above case. The value of ΔT for delaminations from 7 to 12 is more when compared to delaminations 1 to 6 in TT mode and delaminations from 7 to 12 in reflection mode, as shown in Fig. 7. It is also observed that ΔT of delaminations from 7 to 12 is more when they are measured in TT mode. The reason for more ΔT is that the distance covered by thermal waves after passing through delaminations reaching the rear surface is less than delaminations located at the same location in reflection mode. It is also inferred that delamination 7 could not be identified due to insufficient ΔT produced with the applied q of 12000W/m^2.

B. Comparison of Delaminations at Various Depths

Fig. 8 shows the comparison between delaminations located at 0.45mm and 0.6 mm depth in reflection mode. The results reveal that the deeper delaminations produce less ΔT than near-surface delaminations. For example, the delamination 4 produces 0.6571°C at 1 sec with the applied q of 12000 W/m^2 but 0.1526 °C is produced by delamination 10 for the same q.

Similar analysis was made in TT mode, as shown Fig. 9. In this case, it is observed that the deeper delaminations produce more ΔT than near-surface delaminations. For example, the delamination 4 produces 0.1355°C at 1 sec with the same applied q of 12000 W/m^2 but 0.1797°C is produced by delamination 10. The near-surface delaminations might be identified faster with increased ΔT than deeper delaminations in reflection mode but deeper delaminations could also be identified faster with sufficient increased ΔT in TT mode which might not be possible in reflection mode.

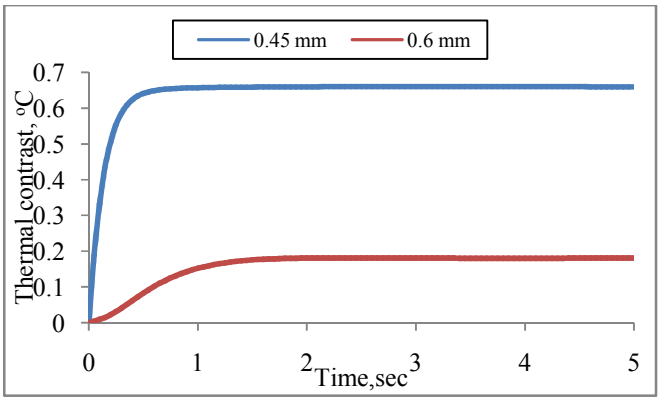

Fig. 8 Comparison of thermal contrast curves with time for delaminations 4 and 10 in reflection mode

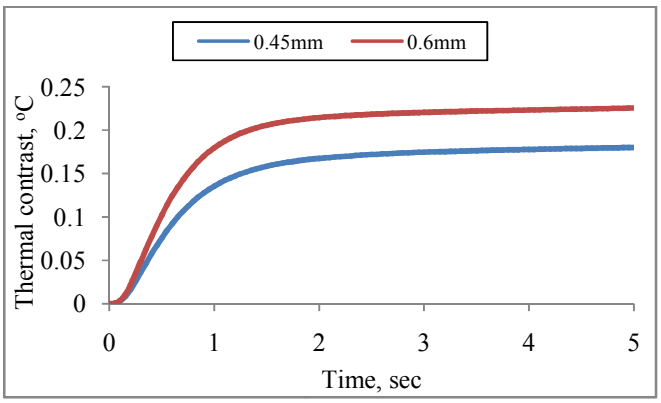

Fig. 9 Comparison of thermal contrast curves with time for delaminations 4 and 10 in TT mode

C. Effect of Applied Heat Flux on Fixed Delamination Size

In the reflection mode, the results shown in Fig. 10 illustrate that ΔT for delamination 6 varies with time for various applied heat fluxes. The thermal curves are similar and equi-spaced one above the other due to constant increase in applied q. For example, delamination 6 produces less ΔT for 1500W/m^2 but it is more when 12000W/m^2 is applied.

Similar behavior is observed in: (i) TT mode and (ii) delaminations located at 0.6mm depth in both modes, as shown in Figs. 11-13. The results conclude that Δ*T* of delaminations is directly proportional to the applied q as per Fourier's law of heat conduction irrespective of mode of observation and delamination locations. The above

investigations also reveal that q required for producing sufficient MRTD to identify delaminations is mainly based on applied q, time, depth and size of delaminations.

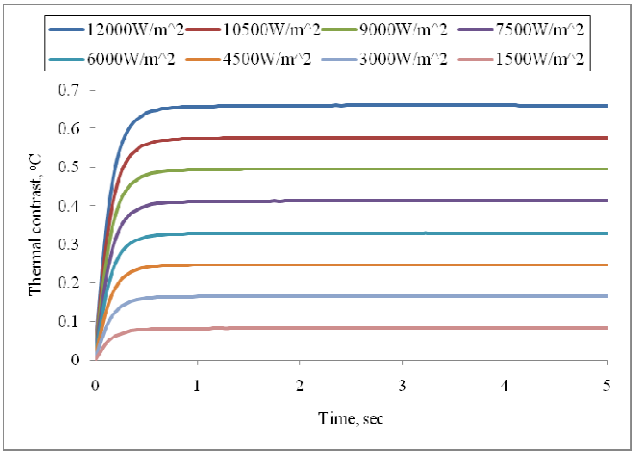

Fig. 10 Thermal contrast curve of delamination 6 with time for various applied q in reflection mode

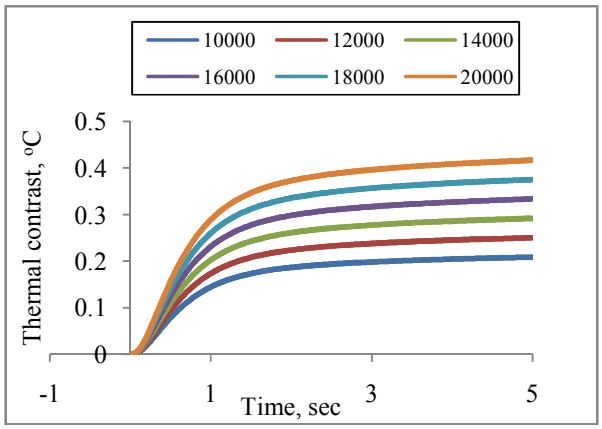

Fig. 11 Thermal contrast curve of delamination 6 with time for various applied heat fluxes (q) in TT mode

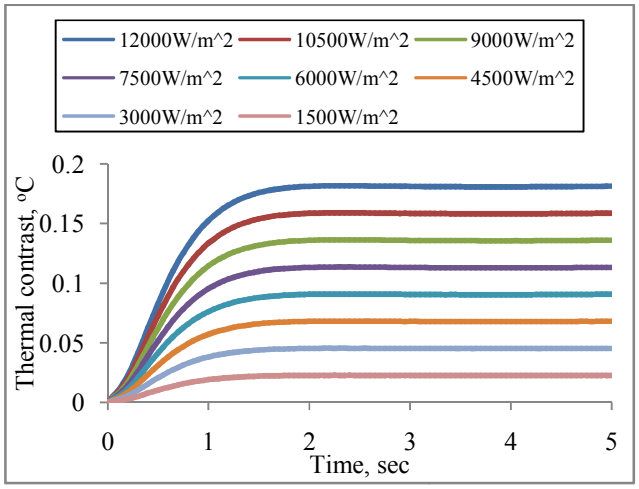

Fig. 12 Thermal contrast curve of delamination 12 with time for various applied q in reflection mode

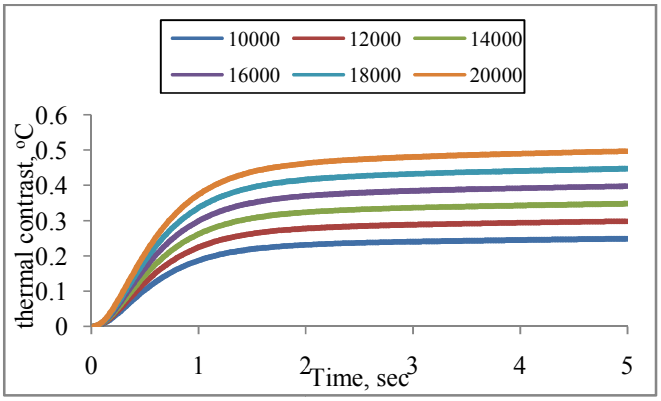

Fig. 13 Thermal contrast curve of delamination 12 with time for various applied heat fluxes (q) in TT mode

D. Heat Requirement Analysis in Reflection Mode

Fig. 14 shows that ΔT at 1 sec for delaminations from 1 to 6 varies linearly with applied heat flux. From results, it is observed that the delaminations from 1 to 6 produce sufficient MRTD for the delamination detection.

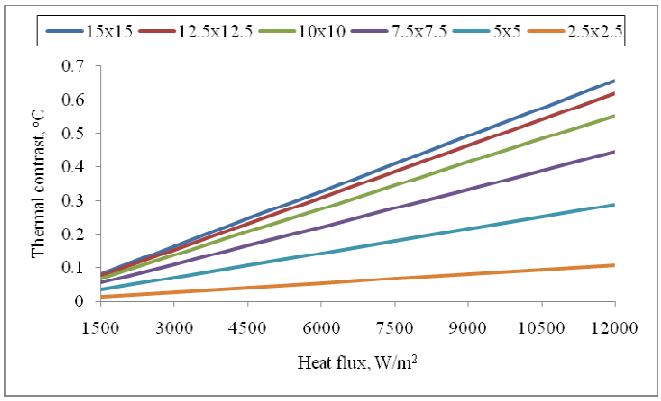

Fig. 14 Thermal contrast curve of delaminations 1 to 6 with q at 1sec

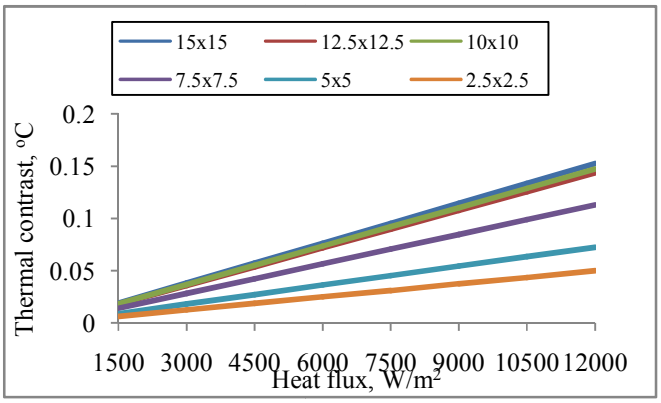

Fig. 15 Thermal contrast curve of delaminations 7 to 12 with q at 1sec

Fig. 15 shows the similar analysis carried for delaminations from 7 to 12. From results, it is observed that delaminations 7 and 8 do not attain the required MRTD with the maximum applied heat of 12000W/m^2 but the delaminations from 9 to 12

produce sufficient MRTD for the effective identification of delaminations. Therefore, the study reveals that the delaminations 7 and 8 could not be identified with the maximum applied q but they might be identified by applying more heat flux. Therefore, the development of a mathematical model through extracted numerical results from simulations might resolve this problem to find the heat requirement for unidentified delaminations.

The optimum heat requirement could be derived through heat requirement analysis by generalized equations for 0.45mm and 0.6mm depth individually.

The optimum heat requirement equation for delaminations 1 to 6 could be obtained by:

$$q = 588719999990.9s^4 - 33960637036.7s^3 + 711903722.2s^2 - 6443275.1s + 23280 \quad (1)$$

The optimum heat requirement equation for delaminations 7 to 12 could be obtained by:

$$q = 615319704135219s^5 - 28384355574544.6s^4 + 477153481794.08s^3 - 3363522224.59s^2 + 6917754.82s + 22335.78 \quad (2)$$

E. Heat Requirement Analysis in TT Mode

Similar heat requirement analysis was carried for delaminations from 1 to 12 in TT mode. The thermal behaviour is shown in Figs. 16 and 17. In this case also, delamination 1 and 2 do not attain the required MRTD with the maximum applied heat of 20000W/m^2 except delaminations from 3 to 6. In addition, the delamination 7 could not be identified within the load conditions considered in this study.

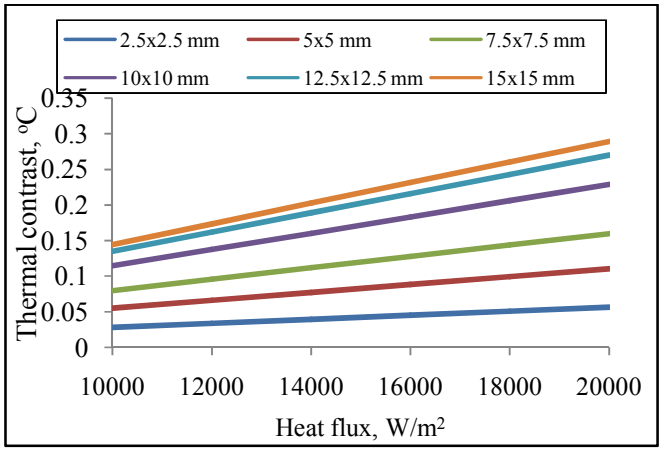

Fig. 16 Thermal contrast curve of delaminations 1 to 6 with q at 1sec

The optimum heat requirement equation for delaminations 1 to 6 could be obtained by:

$$q = -215370240122208s^5 + 10771712005319.8s^4 - 222085253419.75s^3 + 2452892800.65s^2 - 14951034.27s + 45128.22 \quad (3)$$

The optimum heat requirement equation for delaminations 7 to 12 could be obtained by:

$$q = -26613333333.35s^3 + 998000000s^2 - 12309466.67s + 59906 \quad (4)$$

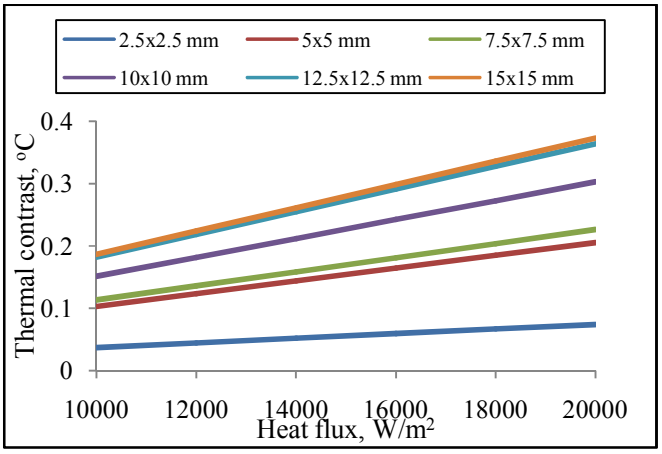

Fig. 17 Thermal contrast curve of delaminations 7 to 12 with q at 1sec

F. Comparison of Heat Requirement

In the reflection mode, from (1) and (2), the delamination 2 and delamination 6 require 4984.088W/m^2 and 1996.011W/m^2 to respond for the presence of delaminations, but 16663.34W/m^2 and 10003.002W/m^2 are required to identify delaminations 8 and 12 respectively. It is understood that delamination 2 is smaller than delamination 6 and delamination 8 is smaller than 12. From results arrived by comparison, it is inferred that smaller and deeper delaminations need more q than larger and near-surface delaminations. From the heat requirement analysis shown in Fig. 18, the optimum q needs to identify unidentified delamination 7 and delamination 8 within the load conditions applied in the analysis as 25015.0022W/m^2 and 16663.3356 W/m^2 respectively.

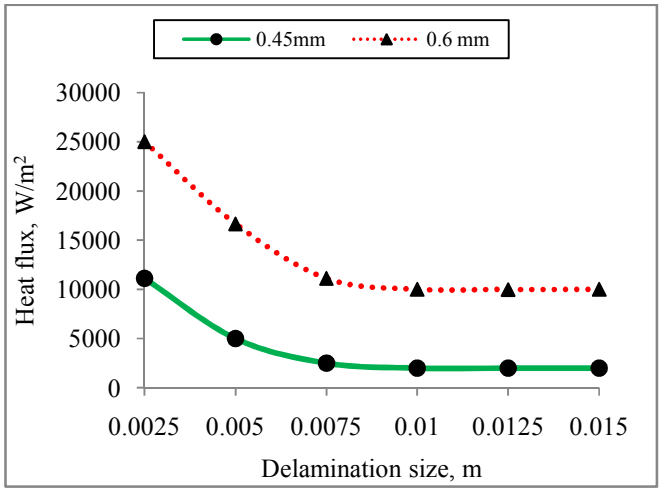

Fig. 18 Comparison of heat requirement for delaminations 1 to 6 and 7 to 12 in reflection mode

Similar to reflection mode, the optimum q is calculated for the delamination 2 as 20002.67W/m^2 which exceeds the maximum q applied in this study and delamination 6 requires 9994W/m^2 to identify the presence of delaminations in TT mode from (3) and (4). The optimum q of 9994W/m^2 and 4997W/m^2 are required to identify delaminations 8 and 12 respectively, as shown Fig. 19. From results arrived by comparison, the smaller and near-surface delaminations need more q to reach MRTD than larger and deeper delaminations. In addition, the unidentified delamination 1 and delamination 7 need the optimum q of 34954W/m^2 and 20010.87 W/m^2 respectively for its effective identification.

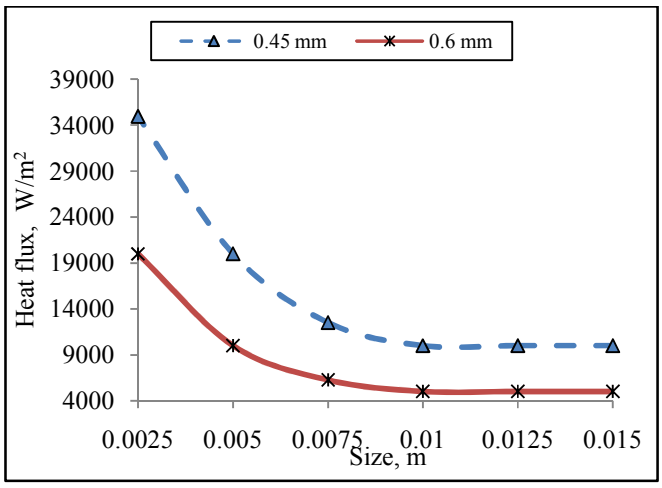

Fig. 19 Comparison of optimum q requirement for delaminations 1 to 6 and 7 to 12 in TT mode

G. Time to Identify Delaminations Analysis in Reflection Mode

One of the main advantages reported about IRT is the fast rate of scanning to detect delaminations. Therefore, for the effective application of SPAT in both modes to analyse delaminations, the analyses could be made on the basis of time to identify delaminations (T) at optimum q. In this analysis also, a mathematical model using extracted numerical results is developed to find T of unidentified delaminations. In the similar way to optimum requirement analysis, T could be derived through generalized equations for 0.45mm and 0.6mm depth individually.

T equation for delaminations 1 to 6 could be obtained by:

$$T = 2592000s^4 - 122933.33s^3 + 2{,}210.20s^2 - 18.09s + 0.08 \quad (5)$$

T equation for delaminations 7 to 12 could be obtained by:

$$T = -2043840s^3 + 76644s^2 - 946.41s + 4.45 \quad (6)$$

From (5) and (6) in reflection mode, the delamination 2 and delamination 6 could be identified at optimum q in 0.03536sec which could not identified within the considered load considered in this study and 0.02657sec respectively but 1.37857sec and 0.5999sec are required to identify delaminations 8 and 12 respectively, as shown in Fig. 20. From these results, it is understood that smaller delaminations 2 and 8 need more T than larger delaminations 6 and 12. It is also observed that smaller near-surface delamination 2 needs 0.03536sec than 0.02657sec of delamination 8. From these two findings, it is concluded that smaller near-surface delaminations located at 0.45 mm depth need less T to reach MRTD than smaller deeper delaminations in reflection mode. T of unidentified delamination 7 is also calculated from the mathematical model as 2.531sec.

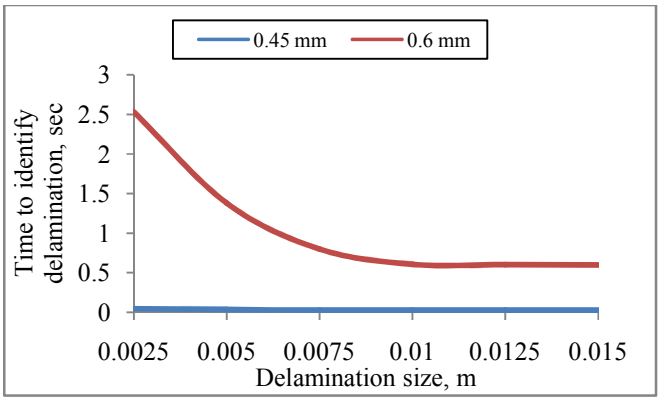

Fig. 20 Comparison of T for delaminations 1 to 6 and 7 to 12 in reflection mode

H. Time to Identify Delaminations Analysis in TT mode

Similar analysis was carried in TT mode also,

T equation for delaminations 1 to 6 could be obtained by:

$$T = 931413333.34s^4 - 43137066.67s^3 + 741506.67s^2 - 5627.75s + 16.41 \quad (7)$$

T equation for delaminations 7 to 12 could be obtained by:

$$T = -106986666.67s^4 + 4576533.33s^3 - 68755.33s^2 + 406.04s - 0.34 \quad (8)$$

In TT mode, from (7) and (8), the delamination 2 and delamination 6 could be identified at optimum q in 1.998sec (unidentified delamination) and 0.3979sec respectively but 0.4765sec and 0.3103sec are required to identify delaminations 8 and 12 respectively. From these results shown in Fig. 21, it is understood that smaller delaminations 2 and 8 need more T than larger delaminations 6 and 12. It is also observed that smaller near-surface delamination 2 needs 1.998sec than 0.4765sec of delamination 8. From these two findings, it is concluded that smaller near-surface delaminations need more T to reach MRTD than deeper delaminations in TT mode. T for unidentified delamination 1 and delamination 7 is calculated from the mathematical model as 13.0399sec and 0.6171sec respectively to identify them at optimum q.

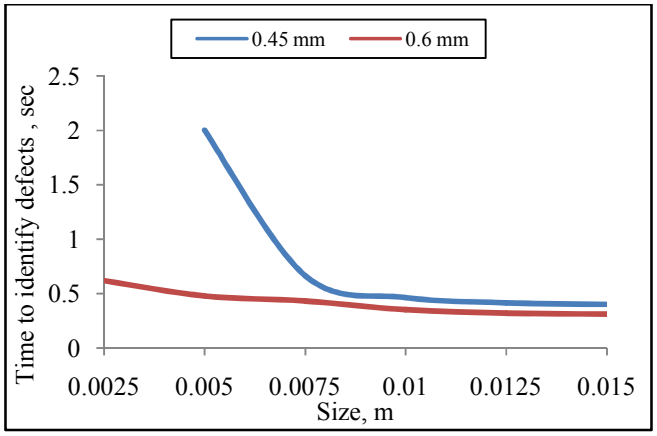

Fig. 21 Comparison of T for delaminations 1 to 6 and 7 to 12

VI. Conclusions

In this study, delaminations present in FML using SPAT method was carried out through developing mathematical models from extracted numerical results. The developed mathematical models allowed analysing the effect of applied heat flux, depth and size of delaminations for deriving the optimum heat requirement and time to identify delaminations. Delaminations respond accordingly by producing its own thermal contrast curve pattern when thermal excitation is applied for numerical simulations in both reflection and TT modes. Numerical results based on SPAT for analysing delaminations provide a good defect resolution; however, numerical results are strongly dependent on surface features and material properties. Generally, larger and near-surface delaminations produce more thermal contrast when compared to smaller and deeper delaminations in reflection mode. Nevertheless, smaller and near-surface delaminations produce less thermal contrast when compared to larger and deeper delaminations in TT mode.

The results conclude that the numerical approach based on SPAT in reflection mode is more suitable for analysing smaller size of near-surface delaminations located at the thermal stimulator side and TT mode is more suitable for analysing smaller size of deeper delaminations located far from thermal stimulator side or near thermal detector/Infrared camera side.

In addition, the mathematical models provide the optimum q and T at the required MRTD to identify unidentified delamination 7 with 25015.0022W/m^2 at 2.531sec and delamination 8 with 16663.3356 W/m^2 at 1.37857sec in reflection mode. In TT mode, delamination 1 with 34954W/m^2 at 13.0399sec, delamination 2 with 20002.67W/m^2 at 1.998sec and delamination 7 with 20010.87 W/m^2 at 0.6171sec could be identified. Results reveal that the numerical approach based on SPAT method could be utilized to analyse delaminations present in FML effectively by developing mathematical models from extracted numerical results by a FEM package.

Acknowledgment

The authors would like to acknowledge Dr. Benny Jospeh, Principal, Vimal Jothi Engineering College, Kerla India, for his kind cooperation & support to provide for the valuable guidelines extended to collect literatures about FML.

References

[1] Ad Vlot and Jan Willem Gunnink, "*Fibre Metal Laminates": An Introduction.* Kluwer Academic Publishers. Springer Netherlands, 2001.
[2] ANSYS, *ANSYS Heat Transfer Manual* for Release 10, 2005.
[3] Avdelidis N. P and Almond D.P, "Transient thermography as a through skin imaging technique for aircraft assembly Modelling and experimental results", *Journal of Infrared Phys. Technol.*, Vol. 45. No. 2, pp. 103-114, 2004.
[4] Avdelidis N.P, Almond D.P, Dobbinson A, Hawtin B.C, Ibarra-Castanedo C and Maldague X, "Aircraft composites assessment by means of transient thermal NDT", *Progress in Aerospace Sciences,* Vol. 40, pp 143–162, 2004.
[5] Guillen and Can, "The influence of cooling rate on the fracture properties of a thermoplastic-based FMLs", *Journal reinforced plastics and composites*, Vol. 21. No. 8, pp. 749-772, 2002.
[6] Hagenbeek M, "Characterisation of Fibre Metal Laminates under Thermo- mechanical Loadings". PhD thesis. Faculty of Aerospace Engineering, 2005, *Delft University of Technology*, pp 224.
[7] Ibarra-Castanedo C, Grinzato E, Marinetti S, Bison P, Genest M, Grenier M, Jean-Marc Piau, Bendada A and Maldague X, "Recent progresses in the inspection of aerospace components by infrared thermography" *17th World Conference on Nondestructive Testing*, 2008, *Shanghai, China,* pp.25-28.
[8] Ibarra-Castanedo1 P, Avdelidis N.P, Grinzato G, Paolo G, Sergio M, Claudiu P, Abdelhakim B and Maldague X, "Delamination detection and impact damage assessment of GLARE by active thermography", *International Journal of materials and Product Technology*, 2011, Vol. 41, pp. 5-16.
[9] Krishnapillai M, Jones R, Marshall I.H, Bannister M, and Rajic N, "NDTE using pulse thermography: Numerical modeling of composite subsurface defects", *J. Composite Structures*, Vol. 75, pp. 241-249, 2006.
[10] Lugin S and Netzelmann U, "A defect shape reconstruction algorithm for pulsed thermography", *NDT&E International*, Vol. 40, pp. 220–228, 2007.
[11] Mabrouki F, Genest M, Shi G and Fahr A, "Numerical modeling for thermographic inspection of fibre metal laminates", *J. NDT and E International*, Vol. 42, pp. 581-588, 2009.
[12] Maldague X, "*Theory and practice of infrared technology for nondestructive testing*" Wiley-Interscience, *New York*. 453 – 525, 2001.

[13] Meola C, Givanni M.C, Squillace A and Vitiello A, "Non-destructive evaluation of aerospace materials with lock-in thermography" *J. Engineering Failure Analysis*, Vol. 13. No. 3, pp. 380-388, 2006.
[14] Mirela S, Ibrarra-Castanedo, Maldague X, Bendada A, Svaic S and Boras I, "Pulse thermography applied on a complex structure sample: comparison and analysis of numerical and experimental results", *IV conferencia Panamericana de END*, *Buenos Aires,* 2007.
[15] Muralidhar C and Arya N.K, "Evaluation of defects in axisymmetric composite structures by thermography", *NDT&E International*, Vol. 26. No. 4, pp. 198-193, 1993.
[16] Muzia G, Rdzawski Z.M, Rojek M, Stabik J and Wróbel G, "Thermographic diagnosis of fatigue degradation of epoxy-glass composites", *Journal of Achievements in Materials and Manufacturing Engineering*, Vol. 24. No. 2, pp. 123-126, 2007.
[17] Omar M, Hassan M, Saito K and Alloo R, "IR self-referencing thermography for detection of in-depth defects", *Journal of Infrared Physics and Technology*, *46*(4), pp 283-289, 2005.
[18] Omar M, Haassan M, Donohue K, Saito K and Alloo R, "Infrared thermography for inspecting the adhesion integrity of plastic welded joints", *NDT and E International*, Vol. 39, pp. 1-7, 2006.
[19] Peter linde, Jürgen pleitner, Henk de boer and Jos sinke, "Numerical and experimental simulation of damage behaviour of fibre metal laminates", *24th international congress of the aeronautical sciences*, ICAS 2004.
[20] Qiaojian Huang, Regez Brad, Krishnaswamy and Sridhar, "The influence of disbond defects on Lamb wave testing in GLARE composites" *Proceedings of the SPIE*, 2010, Vol. 7650, pp. 76502P-76502P-8.
[21] Saintey M B and Almond D P, "Defect Sizing by Transient Thermography II: A Numerical Treatment", *Journal of physics. D, Applied physics*, Vol. 28, pp. 2539-2546,1995.
[22] Speer. and Es-Said. 2004. Applications of an aluminum–beryllium composite for structural aerospace components, *Engineering Failure Analysis*, Vol. 11. No. 6, pp. 895–902.
[23] Sundaravalli S, Vijayaraghavan G.K. and Majumder M.C. "Estimation of required heat input for the evaluation of Disbonds in FMLs Using Thermography", International Conference on Modeling, Optimization and Computing (ICMOC 2010), National Institute of Technology, Durgapur, India, October *28 - 30, 2010*, American Institute of Physics (AIP) Conference Proceedings, Vol. 1298, pp 129-134. ISBN: 978-0-7354-0854-8
[24] Sundaravalli S, Majumder M and Vijayaraghavan G.K "Numerical Analysis of Defects in FML using Through-Transmission Mode of Active Thermography", *Journal of Engineering Trends and Technology*, Vol. 3. No. 3, pp 437-447, 2012.
[25] Timothy B Roth and Ann M. Anderson, "A Light Transmission Based Liquid Crystal Thermography System," *Journal of* Heat Transfer, Vol. 30. No.1, 2008.
[26] Vageswar A, Balasubramaniam K, Krishnamurthy C.V, Jayakumar T and Raj B, "Periscope infrared thermography for local wall thinning in tubes", *NDT&E International, 42* (4), pp 275–282, 2009.
[27] Vijayaraghavan G K, Majumder M.C and Ramachandran K.P, "Quantitative Analysis of Delaminations in GRP Pipes Using Thermal NDTE Technique", *Journal of Advanced Research in Mechanical Engineering*, Vol. 1. No. 1, pp.60-68*,* 2010.
[28] Vijayaraghavan G.K. and Sundaravalli S "Evaluation of Pits in GRP Composite Pipes by Thermal NDT Technique". *Journal of Reinforced Plastics and Composites*, 30 (19), pp 1599–1604, 2011.
[29] Sundaravalli S, Majumder M.C and Vijayaraghavan G.K "*Numerical Analyses of Defects in FML using Through-Transmission Mode of Active THermograpghy*", International journal of Engineering and Technology, 3(3), pp 437-447, 2012.

S. Sundaravalli is currently working as a Faculty in the Department of Mechanical engineering, M.A.M College of Engineering, Trichy, India. An M. Tech in Energy Technology from the Pondicherry engineering College, Pondicherry, she has around fourteen years of teaching experience and currently pursuing Ph D in the National Institute of Technology, Durgapur, India. She has authored 8 text books, such as Engineering Thermodynamics, Design jigs, fixtures and press tools, Manufacturing technology II, Automobile engineering, Renewable sources of energy etc.,

Dr. M C Majumder is a Professor in the Department of Mechanical Engineering and Member Secretary of the Senate, National Institute of Technology, Durgapur, India. He has a PhD from the Indian Institute of Technology, Kharagpur, India. He has guided many Ph D scholars. His prime area of research is Tribology.

Dr. G. K. Vijayaraghavan is currently working as a Principal with Mechanical engineering, Cauvery College of Engineering and Technology, Trichy, India. An M. Tech in Machine Design from the Indian Institute of Technology, Madras, he has around Fifteen years of teaching experience and pursed Ph D in the National Institute of Technology, Durgapur, India. He has authored 14 text books including Design of machine elements, Design jigs, fixtures and press tools, Manufacturing technology, Thermal engineering and Mechatronics.